

Thermocapillary and Magnetohydrodynamic Effects in Modelling the Thermodynamics of Stationary Welding Processes

**Michael HUGHES, Gareth A. TAYLOR
and Koulis PERICLEOUS**

Centre for Numerical Modelling and Process Analysis,
University of Greenwich, London, UK

Tel: (44/0)20 8331 8703, Fax: (44/0)20 8331 8665, E-mail: m.s.hughes@gre.ac.uk

ABSTRACT

A steady state model of heat transport by conduction and convection is extended to include both Marangoni and Lorentz effects. Both effects are investigated with respect to heat transport and solidification in a stationary axisymmetric weld pool.

The PHOENICS implementations of Marangoni and Lorentz effects are validated against individual analytical solutions. Furthermore, the integration of the effects within the fluid dynamics of an axisymmetric weld pool is compared against available data.

KEYWORDS:

Stationary Welding, Fluid Dynamics, Magnetohydrodynamics, Thermocapillary

Version : PHOENICS 2.1.3
Computer : Sun Ultra -5.10 333MHz
Operating System : SunOS 5.6

NOMENCLATURE

B magnetic flux	μ dynamic viscosity
C_p specific heat	ρ density
I electric current	σ electrical conductivity
k thermal conductivity	
p pressure	
T temperature	
u velocity	
V potential difference between electrode and work piece	

INTRODUCTION

In recent years there has been much progress in the understanding of fluid flow and heat transfer phenomena in welding processes [20,10,2]. Essential to the concept of a welding process is the application of a localised heat source in order to reduce the size of the heat affected zone (HAZ) and hence reduce defects such as distortion and residual stress in the workpiece [6].

The interaction of the buoyancy, tensile surface (Marangoni) and electromagnetic (Lorentz) forces (which exist in arc welding processes only), can combine together to produce complex flow patterns. The resulting patterns are dependent on the relative magnitude of the above forces and influence the shapes of both the fusion zone (FZ) and the HAZ. In particular, they can be affected by temperature dependent properties, especially the surface tension coefficient that defines the relative strength and direction of the Marangoni forces [17]. Depending on the value of this coefficient, the Marangoni forces can support natural convection and oppose the Lorentz forces to form a surface flow pattern that is directed radially outwards from the heat source. Therefore producing weld pools which are relatively wide and shallow. Alternatively, the Marangoni forces can act in the same direction as the electromagnetic forces to oppose natural convection, causing a radially inward surface flow direction, with a tendency to give narrow deep weldpools. These effects have been investigated by several authors for various welding processes and materials over the years [12,14]. More recently consideration of these driving forces, in conjunction with free surface models, have been investigated in an attempt to predict the shapes of both FZ and HAZ more accurately [19,20].

Traditionally the modelling of welding has followed two strategies, firstly it is possible to focus on the fluid and thermodynamics local to the weld pool [20,16,23] and secondly it is possible to model the global thermomechanical behaviour of the weld structure [11,4,3]. In the former case only the local geometry of the weld pool and HAZ is considered [20,16,23] and in the latter case a simplified heat source model is employed with heat transfer by conduction only [6,11,4]. A variety of simplified heat source models are now commonly employed in these cases but they are totally reliant on the accuracy of the model parameters that describe the weld pool size and shape [6,4]. These parameters are obtained from a combination of experimental and calculated data.

The objective of this research is to implement and validate established techniques. Therefore providing a firm foundation to develop models for a variety of welding processes, with the final goal being the improvement in accuracy of the above mentioned parameters in order to achieve a consistency between the predictions of the two modelling approaches.

FLUID DYNAMICS AND HEAT TRANSFER

The governing equations for the incompressible fluid flow and heat transfer that can occur in the weld pool are defined as follows;

Mass conservation,

$$\nabla \cdot \mathbf{u} = 0,$$

momentum conservation,

$$\rho \frac{\partial \mathbf{u}}{\partial t} + \rho \nabla \cdot (\mathbf{u}\mathbf{u}) = -\nabla p + \nabla \cdot \mu \nabla \mathbf{u} + \mathbf{S}_u \quad (1)$$

and heat conservation,

$$\rho C_p \frac{\partial T}{\partial t} + \rho C_p \nabla \cdot (\mathbf{u}T) = \nabla \cdot (k \nabla T) + S_T \quad (2)$$

Darcy, used to retard the flow in solid regions, bouyancy and electromagnetic source terms are included in equation (1), respectively, as follows;

$$\mathbf{S}_u = -\frac{\mu}{K} \mathbf{u} + \rho_0 \alpha \mathbf{g} (T - T_0) + \mathbf{J} \times \mathbf{B}$$

where K is calculated from the Karman-Kozeny equation [16], ρ_0 is the reference density, α is the thermal expansion coefficient, \mathbf{g} is the gravity, T_0 is the reference temperature, \mathbf{J} is current density and \mathbf{B} is magnetic flux density.

The energy sources due to phase changes [16] and Joule heating are included in equation (2) as follows;

$$S_T = -\rho \frac{\partial (f_l L)}{\partial t} - \rho \nabla \cdot (\mathbf{u} f_l L) + \frac{|\mathbf{J}|^2}{\sigma},$$

where f_l is the liquid metal fraction, L is the specific latent heat of fusion and σ is electrical conductivity.

Magnetohydrodynamics (MHD)

The current density distribution in the metal is calculated from the electric potential equation as follows;

$$\nabla \cdot (\sigma \nabla \phi) = \nabla \cdot (\mathbf{u} \times \mathbf{B}) + S_\phi \quad (3)$$

The source for the electric potential ϕ is described by the Gaussian current distribution striking the weld pool surface [2],

$$S_\phi = 3 \frac{I}{\pi r_c^2} \mathbf{e}^{-3 \frac{r^2}{r_c^2}}, \quad (4)$$

where r_c^2 is the effective arc radius and I is the current passing through the electrode. It should be noted that in regions where current can escape the workpiece (e.g. external circuits or clamps) a potential of $\phi = 0$ is applied. Once the electric potential has been solved, the electric field \mathbf{E} and current density \mathbf{J} can be recovered using the following;

$$\mathbf{E} = -\nabla \phi \quad \text{and} \quad \mathbf{J} = \sigma \mathbf{E}. \quad (5)$$

In the axisymmetric case, only the aximutual component of the magnetic field is required for the calculation of the Lorentz forces and it can be derived from Ampere's law as follows;

$$B_\theta = \frac{\mu_0}{r} \int_0^r J_z r dr, \quad (6)$$

where μ_0 is the magnetic permeability of free space, J_z is the z component of the current density and r is the radius

Surface Tension Boundary Condition

The top surface of the weld pool is subjected to the following flow boundary condition [16,22];

$$\boldsymbol{\tau} \cdot \mathbf{n} = \nabla_s s = \frac{\partial s}{\partial T} \nabla_s T,$$

where $\boldsymbol{\tau}$ is the flow stress tensor, \mathbf{n} is the unit outward normal of the liquid metal surface, s is the temperature dependent surface tension and ∇_s is the surface gradient operator [22]. In this research the surface tension as a gradient of temperature, is specified as a model parameter, namely the surface tension coefficient. It is important to note that the curvature effects are neglected as a flat weld pool surface is assumed.

Heat Source

A Gaussian heat source distribution is assumed over the surface [20,4], such that

$$q = \frac{3Q}{\pi r_h^2} e^{-3\left(\frac{r}{r_h}\right)^2}, \quad (7)$$

where Q and r_h are the heat input and characteristic heat source radius respectively.

RESULTS

A selection of results are presented which employ the models defined in the previous section.

Marangoni Effects in Weld Pools

Two problems will be considered. The first case is the motion of a liquid resulting from a free surface, where the surface tension is quadratically dependent on temperature [8]. The second case is the inclusion of Marangoni effects in the axisymmetric modelling of weld pools [20]. In both cases reference solutions are available.

Case 1

The thermo-capillary motion of an idealised liquid with surface tension as a quadratic function of temperature is considered. The boundary conditions required for the thermo-capillary analysis are illustrated in Figure 1. In this analysis a 10 by 0.4 aspect ratio is employed with regard to the geometry. This permits the application of a symmetry condition at a finite distance from the region of interest. The region of interest is defined by the cross section x-s, which is close to the boundary $T = T_0$ as illustrated in Figure 1. The constants β and a , define the quadratic relationship of surface tension s to temperature T , and the linear variation of temperature and spatial coordinate X , respectively. The resultant velocity component profiles are plotted in Figures 2 and 3, along the cross section x-s illustrated in Figure 1. As illustrated the results are in good agreement with the analytical solution [8].

Case 2

The stationary and steady state fusion of an aluminium alloy plate, by a heat source defined over a surface is considered. The model for the steady state heat source distribution is

obtained from equation (7). An axisymmetric approximation is assumed, convective and radiative heat loss boundary conditions applied on remainder of the surface, $x > r$. To enable a localised analysis, it is assumed that the boundary conditions away from the axis and the surface can be derived from the analytical solution for an equivalent point heat source [18]. The results from the numerical analysis are illustrated in Figures 4a and 5a with regard to a negative and positive surface tension coefficient, -0.35×10^{-3} and $+0.1 \times 10^{-3}$ kg/(s²K) respectively. The different coefficient values represent different types of alloy and illustrate the material dependent Marangoni effects on the velocity and temperature fields. The temperature fields are contoured in degrees Celsius, and as illustrated by Figure 4a, the shape of the weld pool is broader for the negative gradient case. The change in weld pool shape is related to the different flow patterns that occur in each weld pool. This is illustrated in Figures 4a and 5a. For the negative and positive gradient cases the predominant surface flow is away from and towards the heat source respectively. The convective heat transport is consequently directed towards or away from the axis, resulting in either a deeper or flatter weld pool shape respectively. The results are in good agreement with those obtained by Tsai and Kou [20], which are represented in Figures 4b and 5b. The profiles for the negative case are in general agreement with regard to weld pool shape, temperature field and flow field illustrated in Figures 4a and 4b. Additionally, the results for the positive case, illustrated in Figures 5a and 5b, are also in good agreement, although it should be noted that in the positive case PHOENICS predicts a slightly deeper weld pool shape, which is probably due to the 'rigid-surface' mesh employed.

Lorentz Effects

Two problems are considered, the first case is a three dimensional duct flow problem involving MHD. The second case is the inclusion of MHD in the axisymmetric modelling of weld pools.

Case 3

As a means of validating electric field and Lorentz force calculations, the steady flow of an electrically conducting, viscous, incompressible fluid within a square duct with both parallel perfectly conducting and insulating walls. A constant transverse magnetic field was applied. The problem is illustrated schematically in Figure 6. The combination of parallel pairs of electrically conducting and insulating walls allows a current that will accelerate the flow close to the non-conducting walls whilst retarding it elsewhere. The Hartmann number, represents the ratio of electromagnetic to viscous forces and is defined as $Ha = \sigma |B|^2 l^2 / \mu$, where l is the half width of the duct and μ is the dynamic viscosity of the fluid. As the Hartmann number increases, the electromagnetic forces increase and the flow develops a characteristic M-shape profile as seen in Figure 7. In this case, the standard Navier-Stokes equations were solved, with the addition of a Lorentz force, which was represented as follows;

$$\mathbf{S}_u = \sigma |\mathbf{B}|^2 \left(\frac{\mathbf{E}}{|\mathbf{B}|} + \mathbf{u} \right)$$

where \mathbf{E} was recovered from equation (5). The analytical solution to this problem was initially derived by Hunt [9], and some interesting stability considerations are also provided by Leboucher [13]. A listing of the FORTRAN 77 source code to calculate the analytical pressure gradient is contained in the Appendix. Non-slip boundary conditions were applied to the walls with a constant inlet flow profile. The electrical boundary conditions were applied by enforcing a zero potential at the perfectly conducting walls and zero flux condition at insulating walls. The grid dimensions were 1m x 1m x 10m and both a coarse and finer grid

were employed of cell densities 20x20x20 and 50x50x20 respectively. The analysis was performed for a range of Hartmann numbers and the numerical pressure gradient compared against that calculated from the analytical solution [9]. The pressure gradient was calculated along the centre line, half way down the duct. Comparisons of observed and predicted pressure gradients are shown in Table 1. The numerical results compare well with the analytical predictions indicating correct calculation and implementation of the Lorentz forces in equation (1).

Case 4

The stationary steady state welding of an aluminium plate as specified in case 2, was extended to account for electromagnetic effects within the governing equations. In the original case electromagnetic effects could be neglected as a laser weld was modelled. The case was developed in order to examine the qualitative effects of introducing electromagnetic effects into the original model. The Q1 and ground files are included in the Appendix and case 2 can be recovered from these by commenting the electromagnetic patches in the Q1. A current source as specified by equation (4), was applied to the top of the workpiece, with an effective radius of 1mm and a magnitude of 200 Amperes. An equivalent heat source was applied as specified in the original case, in order to examine the change in the flow profiles with the addition of Lorentz forces. It should be noted however, that the net power applied to the workpiece (Q in equation (7)), would usually be estimated as $IV\eta$, where I is electrode current, V is potential difference between electrode and workpiece and η is an efficiency factor. Additionally a zero electric potential boundary condition was applied to the circumferential surface of the domain to complete a circuit and allow current to pass through. Magnetic flux density was calculated using equation (6).

The results from the analysis are presented for qualitative comparison of negative and positive surface tension gradients respectively in Figures 8a and 8b. The Lorentz forces act in the opposite direction to natural convection, and depending on the magnitude of the applied current are usually the most dominant of the three forces. Figure 8a shows the Lorentz force acting in the opposite direction to Marangoni and natural convection. The flow patterns can vary quite significantly depending on the relative strengths of the forces. The shear flow on the surface of the pool is driven by Marangoni forces, and the bulk recirculatory flow in the upper region of the pool is assisted by the Lorentz forces. This is because the Lorentz forces are decreasing significantly with depth and are therefore promoting an increasing acceleration in the upper region of the pool where they are strongest. Alternatively, in the lower region of the pool, where the Lorentz forces are weaker, the viscous shear reverses the direction of the recirculating flow. In this region the flow is significantly less than in the upper part of the pool, in fact it seems quite stagnant in comparison. However it should be noted that this is dependent on the magnitude of the Lorentz forces.

Figure 8b shows the effect of combining the Lorentz forces with a positive surface tension coefficient. In this case the effect is quite intuitive, since the Lorentz forces are acting in the same direction as the Marangoni forces. As in the original case the surface flow is forced radially inwards towards the center of the heat source. This is due to the combination of the forces and is to a greater extent than in Figure 5a. The resulting weld pool is therefore similar to that shown in Figure 5a, but with a deeper penetration. Continuity ensures that the return path for the flow in the weld pool is also wider than in Figure 5a.

FURTHER RESEARCH

It is planned to extend the principles investigated in this study to general 3D, non-stationary welding processes. There are a number of methods for modelling non-stationary welding processes depending upon the reference frame associated with the heat source. Essentially, the methods are Eulerian and the heat source is stationary [1,5], or Lagrangian and the heat source is moving [3,21]. The Lagrangian approach is reasonably accurate for simplified heat sources moving with a constant velocity [7], but it is not suitable when modelling the fluid dynamics of a weld pool associated with a moving heat source. Therefore, further research will concentrate on the development of Eulerian techniques to account for heat source motion. This will facilitate the localised modelling of the fluid dynamics associated with a moving weld pool. Additionally, an investigation is planned to supply parameters to simplified heat source models that can better describe the digging and convective temperature distribution resulting from the local weld pool dynamics [6,7,21]. This will provide consistency between the simplified heat source models and the fluid dynamics of the weld pool. Such methods allow the complete modelling of the welding process, without resort to the expense of a flow simulation.

It is important to note that the Biot-Savart law could be used as an alternative to equation (6), which is used to calculate the magnetic field. In which case the details of the external components, such as the electrode would need to be considered for the accurate modelling of the magnetic field.

CONCLUSION

The two cases 1 and 3, have provided sufficiently accurate comparisons to the analytical solutions to validate the calculation and integration of the Marangoni and Lorentz forces. The axisymmetric weld studied in case 2 provided favourable agreement with results presented by Tsai and Kou [20]. Introduction of the Lorentz forces to this case has given interesting insights into the nature of the flow when electromagnetic effects are considered.

REFERENCES

1. CHEN, X., BECKER, M., and MEEKISHO, L.,(1998),“Welding analysis in moving coordinates.”, In H. Cerjak, Editor, *Mathematical Modelling of Welding Phenomena* 4, 396-410.
2. EL-KADDEH, N., ARENAS, M., and ACOFF, V.L.,(1999),“Heat Transfer and Fluid Flow in stationary GTA welding of γ -TiAl based alloys: effect of Thermocapillary flow”, Second International Conference on CFD in the Minerals and Process Industries, CSIRO, Melbourne, Australia.
3. FENG, Z. CHENG, W. and CHEN, Y.,(1988),“Development of new modelling procedures for 3D welding residual stress and distortion assesment”, Cooperative Research Program, **SR9818**.
4. FRIEDMAN, E.,(1975),”Thermodynamic analysis of the welding process using the Finite Element Method”, *Journal of Pressure Vessel Technology, Trans, ASME*, **97**, 206-213.
5. GOLDAK, J., BREIGUINE, V. and DAI, N.,(1995),“Computational Weld Mechanics: A Progress Report on Ten Grand Challenges”, In H. B. Smartt, J. A. Johnson and S. A. David, editors, *Trends in Welding Research – IV*, 5-11.
6. GOLDAK, J., CHAKRAVARTI, A. and BIBBY, M.,(1984),“A New Finite Element Model for Welding Heat Sources”, *Met. Trans. B*, **15B**, 299-305.
7. GOLDAK, J., BIBBY, M.,MOORE, J,HOUSE, R, PATEL, B.,(1986),”Computer Modelling of Heat flow in Welds”, *Met. Trans. B*, **17B**, 587-600

8. GUPALO, Y. P. and RYAZANTSEV, Y. S.,(1989),“Thermocapillary motion of a liquid with a free surface with nonlinear dependence of the surface tension on the temperature”, Fluid Dynamics, (English translation), **23:5**, 752-757..
9. HUNT, J.C.R.,(1965),”Magnetohydrodynamic flow in rectangular ducts”,J. Fluid Mech., **21:4**, 577-590.
10. KIM, W.H., FAN, H.G. and NA, S.J.,(1997),“Effect of various driving forces on heat and mass transfer in arc welding”, Numer. Heat Transfer Part A, **32**,633-652
11. KISELEV, S.N., KISELEV, A.S., KURKIN, A.S., ALADINSKII, V.V. and MAKHANEV, V.O.,(1999),“Current Aspects of Computer Modelling Thermal and Deformation Stresses and Structure Formation in Welding and Related Technologies”, Welding International , **13-4**, 314-322.
12. KOU, S. and SUN, D.K.,(1985),“Fluid Flow and Weld penetration in stationary arc welds”, Metall, Trans A, **16A**, 203-213.
13. LÉBOUCHER, L.(1999),“Monotone Scheme and Boundary Conditions for Finite Volume Simulation of Magnetohydrodynamic Internal flows at high Hartmann Number”, J.Comp. Phys.,**150**,181-198.
14. OREPER, G.M. and SZEKELY, J.,(1984), “Heat and fluid flow phenomena in weld pools”, J.Fluid. Mech., **147**, 53-79.
15. PAUL, A. and DEBROY, T.,(1988),”Prediction of Marangoni convection heat transfer and surface profiles during laser welding”,Modeling and Control of Casting and Welding processes IV, The Metallurgical Society, Warrendale, PA, 421-431.
16. PERICLEOUS, K. and BAILEY, C.,(1995),“Study of Marangoni phenomena in laser-melted pools”. In J. Campbell and M. Cross, editors, Modeling of Casting, Welding and Advanced Solidification Processes - VII, 91-100.
17. RADAJ, D., (1992),”Heat Effects of Welding”,Springer-Verlag, ISBN 0-387-54820-3.
18. ROSENTHAL, D., (1946), “The Theory of Moving Sources of Heat and Its Application to Metal Treatments.”, Trans. ASME, **68-11**, 849-866.
19. THOMPSON, M.E., and SZEKELY, J.,(1989),“The transient behaviour of weld pools with a deformed free surface”,J.Heat Mass Transfer, **32**, 1007-1019.
20. TSAI, M.C., and SINDOU K.,(1989),“Marangoni convection in weld pools with a free surface”, Int. J. Num. Methods Engrg., **9**, 1503-1516.
21. VOSS, O., DECKER, I., and WOHLFAHRT, H.,(1998),“Consideration of microstructural transformations in the calculation of residual stresses and distortion of larger weldments.”, In H. Cerjak, Editor, Mathematical Modelling of Welding Phenomena 4, 584-596.
22. WHEELER, D., BAILEY, C. and CROSS, M.,(1999),“Numerical modelling and Validation of Marangoni and Surface Tension Phenomena Using the Finite Volume Method”, Int. J. Num. Methods in Fluids, **212-B**, accepted for publication.
23. ZACHARIA, T., DAVID, S.A., VITEK, J.M. and KRAUS H. G.,(1991),“Computational modelling of stationary gas-tungsten-arc weld pools and comparison to stainless steel 304 experimental results”, Met. Trans B, **22B**, 243-257.

$$\frac{\partial T}{\partial Y} = 0, \quad \mu\rho \frac{\partial u_x}{\partial Y} = \frac{\partial s}{\partial X} = \beta(T - T_0) \frac{\partial T}{\partial X}$$

$T = T_0$ x-s (X = .625m) Symmetry
 $X = 0$ $X = 10$
 $T = T_0 + aX, \quad u_x = u_y = 0$

Figure 1: Thermo-capillary boundary conditions

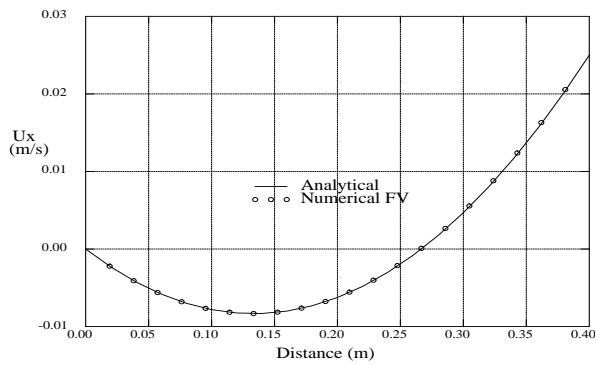


Figure 2: X component velocity profile

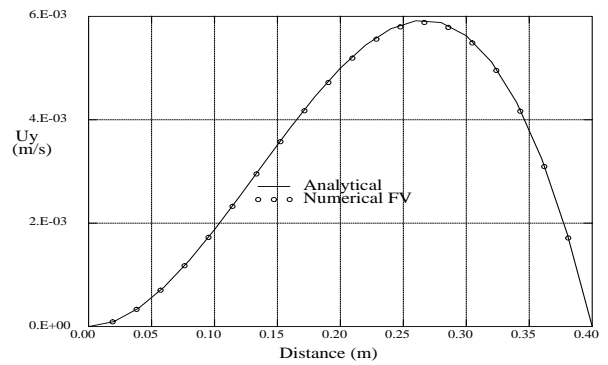


Figure 3: Y component velocity profile

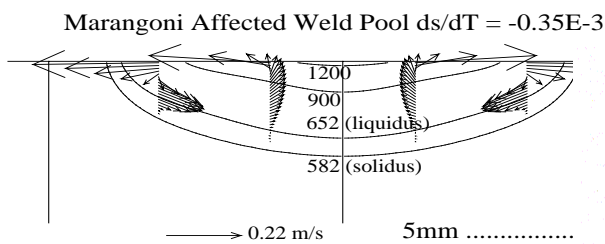


Figure 4a: Negative: Temperature and flow fields

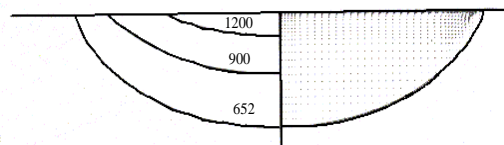


Figure 4b: Negative: Temperature and flow fields [8]

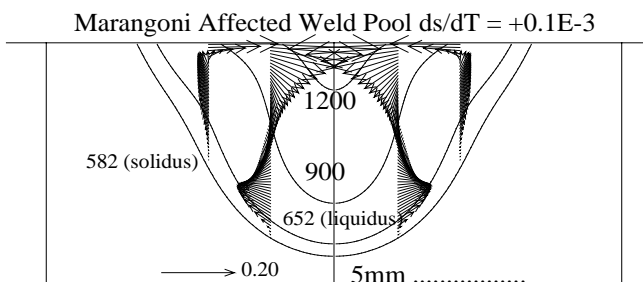


Figure 5b: Positive: Temperature and flow fields [8]

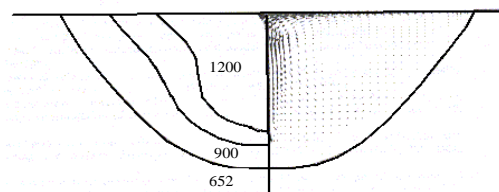


Figure 5a: Positive: Temperature and flow fields

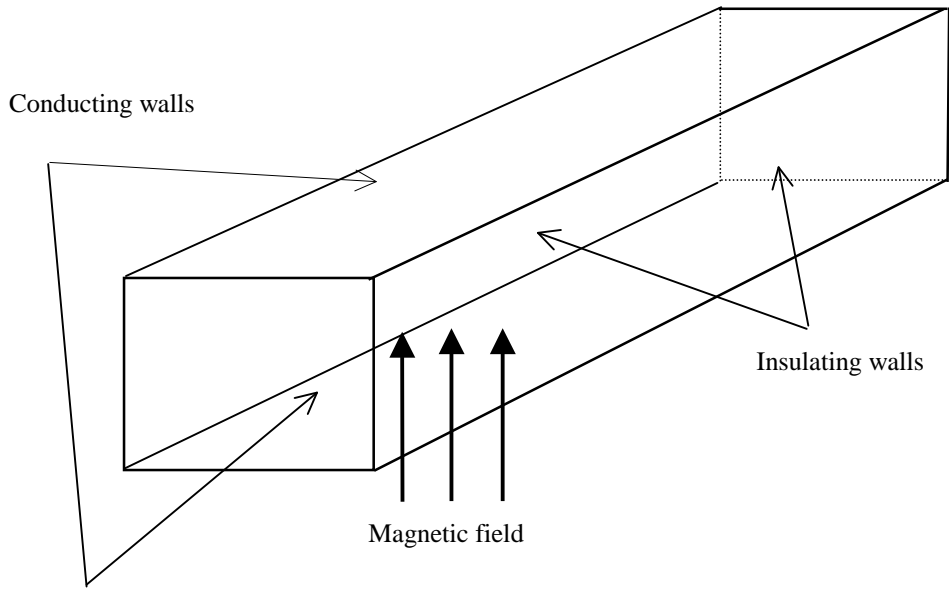


Figure 6: Magnetic duct flow schematic

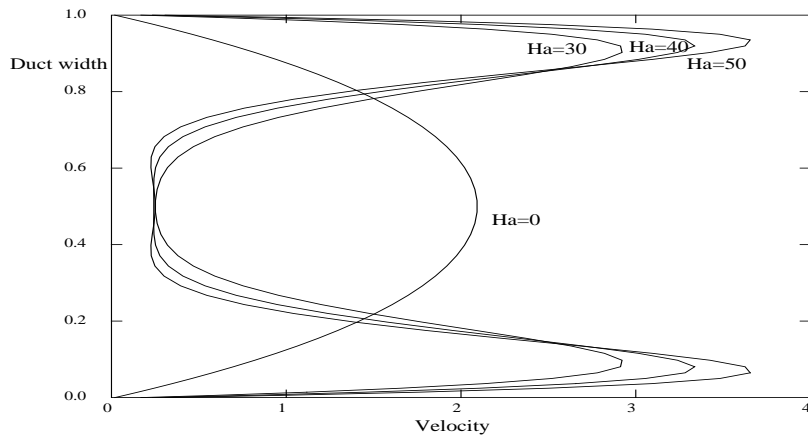


Figure 7: Profiles of Magneto hydrodynamic duct flow

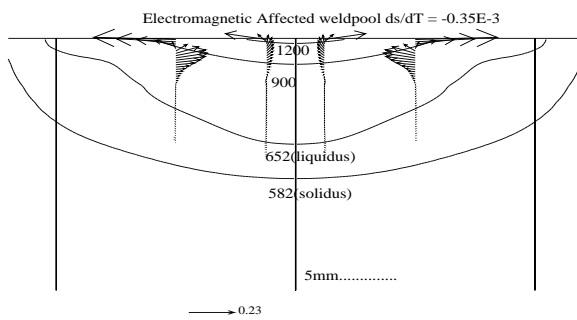


Figure 8a: Negative surface tension and Lorentz forces.

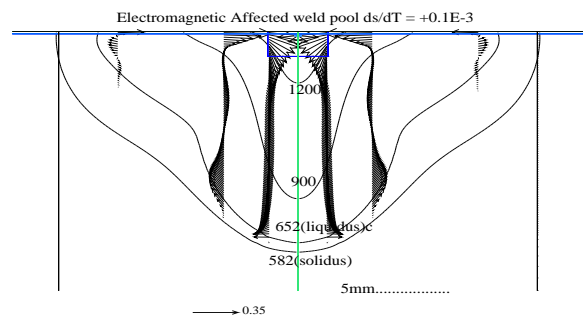


Figure 8b: Positive surface tension and Lorentz forces.

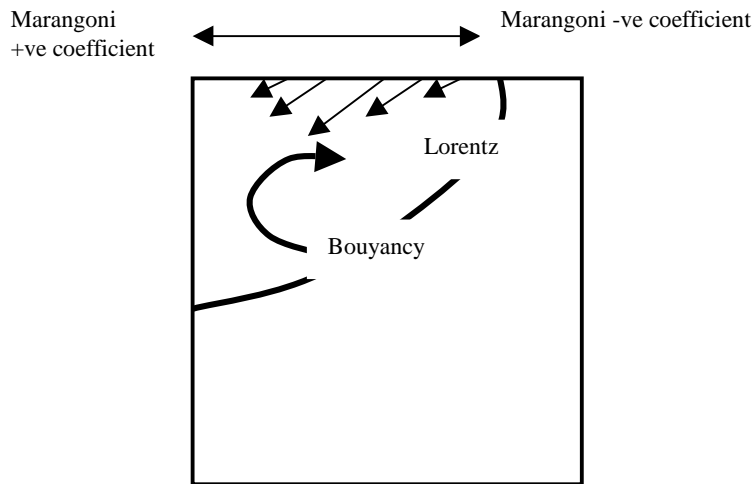


Figure 9: Relative direction of the affecting Forces

Hartmann No.	M=30	M=40	M=50
Analytical	0.397	0.359	0.331
Coarse Mesh	0.406	0.381	0.368
Fine Mesh	0.407	0.354	0.331

Table 1 Analytical vs Numerical Pressure gradients for Case 3

APPENDIX

MHD duct: analytical solution code

```
{Analytical solution program}
c Exact solution of Hartmann flows in rectangular channels.
c From Hunt, J.C.R, 1965, J. Fluid Mech., vol. 21, pp 557-590.

c Compute flow rate Q from equation (28) and pressure drop from
c equations unnumbered equations between equations (8) and (9).

program hunt

implicit none
real*8 M,pi,alpha,k,r1k,r2k,Q,Q1,Q2,Q3,gradP
integer k
write(*,('enter a value for the Hartmann number ',*))
read(*,*) M
pi = 4.*atan(1.)
Q = 0.

do k = 0,500
alpha = (real(k)+0.5)*pi
r1k = 0.5*(+M*sqrt(M**2+4.*alpha**2))
r2k = 0.5*(-M*sqrt(M**2+4.*alpha**2))
Q1 = 8./(alpha**4)
Q2 = r2k*tanh(r1k)/(r1k*sqrt(M**2+4.*alpha**2))
Q3 = r1k*tanh(r2k)/(r2k*sqrt(M**2+4.*alpha**2))
Q = Q + Q1*(1.+Q2-Q3)
gradP = 4./Q/M**2
write(*,('k =',i3,8x,'Q =',f13.10,8x,'gradP =',f13.10))
& k,Q,gradP
enddo

end
```

Q1 file

```

TALK=T;RUN( 1, 1);VDU=X11-TERM
IRUNN = 1 ;LIBREF = 166
*****
Group 1. Run Title
TEXT( Surf tension effects on weld (-ve, g ) )
*****
Group 2. Transience
STEADY = T
*****
Groups 3, 4, 5 Grid Information
* Overall number of cells, RSET(M,NX,NY,NZ,tolerance)
RSET(M,1,100,100 ,1.000E-05)
* Set overall domain extent:
* xulast yvlast zwlast name
XSI= 3.000E-02;YSI= 1.000E-02;ZSI= 1.800E-02;RSET(D,CHAM )
* Set objects: x0 y0 z0
* dx dy dz name
XPO= 0.000E+00;YPO= 0.000E-03;ZPO= 1.3E-02
XSI= 3.000E-02;YSI= 5.000E-03;ZSI= 5.0E-03;RSET(B,B1 )
* Modify default grid
RSET(X,1,1,1.000E+00)
RSET(Y,1,80,1.000E+00)
RSET(Y,2,20 ,1.000E+00)
RSET(Z,1,30 ,1.4000E+00)
RSET(Z,2,90 ,1.000E+00)
* Cylindrical-polar grid
CARTES=F
STEADY=T

REAL(CPLIQ,KLIQ)
REAL(LIQ0,tPOOL)

CPLIQ=1066.;KLIQ=108.
TLIQ0=652;TPOOL=2000

***** solidification constants
REAL(LAT,GBIGA,GLITA,TLQUS,TSOL,TREF)
REAL(GRVTY,BETA)
---
--- LAT --> latent heat of solidification
--- TLQUS --> liquidus temp
--- TSOL --> Solidus temp
--- TREF --> temperature reference
LAT=3.95E5;GBIGA=1.6E3;GLITA=1E-10
TLQUS=652
TSOL=TLQUS-70.0
TREF=(TLQUS + TSOL)/2.0
GRVTY=-9.81
BETA=1.E-4
---
*** K-epsilon model
TURMOD(KEMODL)
STORE(GENK)

SOLUTN(C1,Y,Y,Y,P,P,P)
TERMS(C1,N,N,P,P,P,P)

SOLUTN(P1,Y,Y,Y,P,P,P)
SOLVE(V1,W1,H1)
TERMS(H1,N,P,P,P,P,P)
NAME(C2)=LATH
NAME(C3)=LIQF
NAME(C4)=SOLF

**** lath=latent heat within liquid per unit liq. mass = liqf*lat

STORE(LATH,LIQF,SOLF)
STORE(TMP1,C10,C11,C12,C20,C14,C15,C16,C17,C18,C19)
STORE(PRL)

PRNDTL(C1)=RHO1*ENUL*1.0/1.0
FIINIT(C1)=1.0
DIFCUT=0

RHO1=2700
ENUL=1e-3/2700.
TMP1=GRND2
TMP1B=1/CPLIQ

PRNDTL(H1)=RHO1*ENUL*CPLIQ/KLIQ
PRNDTL(H1)=GRND1

FIINIT(P1)=0
FIINIT(V1)=0
FIINIT(W1)=0
FIINIT(H1)=CPLIQ*TSOL
FIINIT(TMP1)=TSOL
FIINIT(LATH)=0.0
FIINIT(LIQF)=1.0
FIINIT(SOLF)=0.0

INIADD=F

***initialise the weldpool

PATCH (POOL,INIVAL,1,NX,1,10,NZ-10,NZ,1,1)
INIT(POOL,LIQF,0.0,1.0)
INIT(POOL,SOLF,0.0,0.0)

Boundary Conditions
-----
(1)Shear stress at free surface
PATCH(TAU,HIGH,1,NX,1,NY,NZ,NZ,1,LSTEP)
COVAL(TAU,V1,FIXFLU,GRND)
TAU=SKIP

(2)Pressure ref.
PATCH(NWP,CELL,1,NX,1,1,NZ-1,NZ-1,LSTEP)
COVAL(NWP,P1,FXFP,0)
COVAL(NWP,H1,ONLYMS,SAME)

(4)Temperature source
PATCH(GAUSS,HIGH,1,NX,1,NY,NZ,NZ,1,LSTEP)
COVAL(GAUSS,H1,FIXFLU ,GRND )

(5)current source
PATCH(GAUSSJ,HIGH,1,NX,1,NY,NZ,NZ,1,LSTEP)
COVAL(GAUSSJ,C1,FIXFLU ,GRND )

*** Cold far boundary (0.03m away)
PATCH(FAR SIDE,NWALL,1,NX,NY,NY,1,NZ,1,LSTEP)
COVAL(FAR SIDE,H1,1./PRNDTL(H1),GRND)
farside=skip

PATCH(NH1,cell ,1,NX,NY,NY,1,NZ,1,LSTEP)
COVAL(NH1,H1,FIXVAL,CPLIQ*150)
nh1=skip

***Ambient air below
PATCH(BOTTOM,LWALL,1,NX,1,NY,1,1,1,LSTEP)
COVAL(BOTTOM,H1,1./PRNDTL(H1),GRND)
lh=skip

***Ambient air above
PATCH(HH,HIGH,1,NX,56 ,NY,NZ,NZ,1,LSTEP)
COVAL(HH,H1,8.5/CPLIQ,CPLIQ*25 )

***Radiative heat loss
PATCH(HRAD,HIGH,1,NX,64,NY,NZ,NZ,1,LSTEP)
COVAL(HRAD,H1,GRND,GRND)
hrad=skip

*** bc for electric potential
PATCH(END,NWALL, 1,1,NY,NY,1,NZ,1,LSTEP)
COVAL(END,C1,1/PRNDTL(C1),0,0)

(6) LATENT HEAT SOURCE
---- FIX TRANSIENT PART, FIRST
PATCH(DELH, VOLUME, 1,NX, 1,NY, 1,NZ, 1,LSTEP)
COVAL(DELH, H1, FIXFLU, GRND)
DELH=skip
----
---- FIX CONVECTIVE PART
PATCH(CON, CELL, 1, NX, 1,NY, 1,NZ, 1,LSTEP)
COVAL(CON, H1, FIXFLU, GRND)
----
---- SET BOUSSINESQ SOURCE FOR BOUYANCY (NATURAL
CONVECTION)
PATCH(BSQ, VOLUME, 1,NX, 1,NY, 1,NZ-1, 1,LSTEP)
COVAL(BSQ, w1, FIXFLU, GRND)
bsq=skip
----
---- FIX DARCY TERM FOR SIMULATING POROSITY
---- STOP VELOCITY WHEN THE CELL IS FULLY SOLIDIFIED.
PATCH(DARz, volume,1,NX, 1,NY, 1,NZ-1, 1,LSTEP)
COVAL(DARz, w1, GRND, 0.0)
darz=skip
PATCH(DARy, volume, 1,NX, 1,NY-1, 1,NZ, 1,LSTEP)
COVAL(DARy, V1, GRND, 0.0)
dary=skip

PATCH(LORENTZ,VOLUME,1,1,1,NY,1,NZ,1,LSTEP)
COVAL(LORENTZ,V1,FIXFLU,GRND)
COVAL(LORENTZ,W1,FIXFLU,GRND)
Lorentz=skip

PATCH(LORHEAT,VOLUME,1,1,1,NY,1,NZ,1,LSTEP)
COVAL(LORHEAT,H1,FIXFLU,GRND)
Lorheat=skip

LITER(C1)=100

RESREF(W1)=1E-10
RESREF(V1)=1E-10
RESREF(H1)=1E-10*1E3
RESREF(P1)=1E-10

RELAX(KE,FALSDT,.01)
RELAX(EP,FALSDT,.01)

```

```

RELAX(W1,FALSDT,.001)
RELAX(V1,FALSDT,.001)
RELAX(P1,LINRLX,.4)
RELAX(H1,FALSDT,1000)
RELAX(C1,FALSDT,1000)
(DS/DT = const.)
RG(1)= 0.1e-3
RG(11)=tliq0;rg(12)=cpliq
RG(13)=kliq
RG(14)=LAT;RG(15)=GBIGA;RG(16)=GLITA;RG(17)=TLQUS
RG(18)=TSOL;RG(19)=TREF;RG(20)=GRVTY;RG(21)=BETA
RG(22)=ENUL
  Relaxation term for LIQF
RG(23)=0.5
  net power into the system
RG(25)=1800
  effective radius of gaussian heat source
RG(26)=0.004
  stephan-Boltzman constant
RG(27)=5.7E-8
  emmissivity
Rg(28)=0.19
  ambient temperature
RG(29)=25.

```

current supplied

```

RG(30)=200.
  effective current radius
RG(31)=0.004
  electrical conductivity
RG(32)=1.E+6
  magnetic permeability of free space
RG(33)=1.2566E-6
  radius of domain
RG(34)=0.01

```

```

OUTPUT(P1,Y,Y,Y,Y,Y)
OUTPUT(W1,Y,Y,Y,Y,Y)
OUTPUT(V1,Y,Y,Y,Y,Y)
OUTPUT(LIQF,Y,Y,Y,Y,Y)
OUTPUT(SOLF,Y,Y,Y,Y,Y)
OUTPUT(TMP1,Y,Y,Y,Y,Y)
OUTPUT(C1,Y,Y,Y,Y,Y)

```

```

TSTSWP=-1
LSWEEP=1000
IXMON=1
IYMON=5
IZMON=220
STOP

```

Ground.f file

```

C
C--- GROUP 1. Run title and other preliminaries

```

```

1001 CONTINUE
CALL MAKE(YG2D)
CALL MAKE(YV2D)
CALL MAKE(ZGNZ)
CALL MAKE(DYV2D)

```

```

C
RHOLIQ=RHO1
TLIQ=RG(11)
CPLIQ=RG(12)
AKLIQ=RG(13)
GLAT = RG( 14 )
GBIGA = RG( 15 )
GLITA = RG( 16 )
TLQUS = RG( 17 )
TSOL = RG( 18 )
TREF = RG( 19 )
GRVTY = RG( 20 )
BETA = RG( 21 )

```

```

C Add viscosity to Darcy term
RVISCO = RG(22)

```

```

C--- GROUP 9. Properties of the medium (or media)C

```

```

C * ----- SECTION 7 -----
C For PRNDTL( )LE.GRND--- laminar PRANDTL nos., or diffusivity
L0LAM=L0F(LAMPR)
L0SOL=L0F(INAME('SOLF'))
C L0LIQF=L0F(INAME('LIQF'))
DO IX=1,NX
DO IY=1,NY
ICELL=IY+(IX-1)*NY
IF(F(L0SOL+ICELL).GE.0.995)THEN
  F(L0LAM+ICELL)=1e-3*1066./168.
ELSE
  F(L0LAM+ICELL)=1e-3*1066./108.
ENDIF
ENDDO
ENDDO

```

```

C--- GROUP 13. Boundary conditions and special sources

```

```

C          Index for Coefficient - CO
C          Index for Value - VAL
C----- SECTION 1 ----- coefficient = GRND

```

```

C DARCY SOURCE TERM- patches darx, dary, etc

```

```

c IF(NPATCH(1:3),EQ,'DAR') THEN
c L0CO=L0F(CO)
c L0VEL=L0F(INDVAR)
c ILAT=INAME('LATH')
c L0LAT=L0F(ILAT)
c L0LATH=L0F(HIGH(ILAT))
c INEXT=1
c IF(INDVAR.EQ.U1)INEXT=NY
c DO 1301 IX = IXF,IXL
c IXADD=(IX-1)*NY
c DO 1301 IY = IYF,IYL
c ID=IXADD+IY
c F(L0CO+ID)=0.0
c IF(INDVAR.NE.W1)GAVE=0.5*(F(L0LAT+ID)+F(L0LAT+ID+INEXT))
c IF(INDVAR.EQ.W1)GAVE=0.5*(F(L0LAT+ID)+F(L0LATH+ID))
c GLAMDA= GAVE / GLAT
c F(L0CO+ID)=GBIGA*(1.0-GLAMDA)**2/(GLAMDA**3 + GLITA)
c1301 CONTINUE
c END IF

```

```

C Different method to above

```

```

IF(NPATCH(1:3),EQ,'DAR') THEN
I0CO = L0F(CO)
I0LFN = L0F(INAME('LIQF'))
I0SOL = L0F(INAME('SOLF'))
I0C10 = L0F(C10)
DO IX=1,NX
DO IY=1,NY
ICELL = IY + (IX-1)*NY
FVAL=(MAX(F(L0LFN+ICELL),1.e-6)**3)/
& (MAX(F(L0SOL+ICELL),1.e-6)**2)
RPERM = 1E-10*(FVAL+1E-6)
F(L0CO+ICELL)= RHO1*RVISCO/RPERM
F(L0C10+ICELL)= RHO1*RVISCO/RPERM
ENDDO
ENDDO
ENDIF

```

```

IF(NPATCH(1:4),EQ,'HRAD')THEN
C RG(27)=SIGMA
C RG(28)=EMMISSIVITY
C RG(29)=AMBIENT TEMPERATURE DEG C
L0CO=L0F(CO)
L0C12=L0F(C12)
L0T=L0F(INAME('TMP1'))

```

```

DO IX=IXF,IXL
DO IY=IYF,IYL
ICELL = IY + (IX-1)*NY
F(L0CO+ICELL)=RG(27)*RG(28)
& *(RG(29)**2 + F(L0T+ICELL)**2) *
& (F(L0T+ICELL)+RG(29))
F(L0C12+ICELL)=F(L0CO+ICELL)
ENDDO
ENDDO
ENDIF

```

```

C----- SECTION 13 ----- value = GRND

```

```

C Variable Temperature down the length of the vessel

```

```

IF (NPATCH(1:7),EQ,'FAR SIDE')THEN
I0VAL=L0F(VAL)
C Cell center distances from Z=0.0 plane
DO IX=IXF,IXL
DO IY=IYF,IYL
ICELL= IY+(IX-1)*NY
C Should really be cpsol, but cpliq=cpsol in this case !!
F(L0VAL+ICELL)=(-5444.4*GZG(IZ)+205.)*CPLIQ
ENDDO
ENDDO
ENDIF

```

```

C Variable Temperature along the bottom of the vessel

```

```

IF (NPATCH(1:6),EQ,'BOTTOM')THEN
I0VAL=L0F(VAL)
C Cell center distances from Y=0.0 plane
I0dy=I0F(yg2d)
DO IX=IXF,IXL
DO IY=IYF,IYL
ICELL = IY+(IX-1)*NY
C Should really be cpsol, but cpliq=cpsol in this case !!
F(I0VAL+ICELL)=(-1100*F(L0DY+ICELL)+118.)*CPLIQ
ENDDO
ENDDO
ENDIF

```

```

C Gaussian heat source
IF(NPATCH(1:5).EQ.'GAUSS') THEN
  I0VAL = L0F(VAL)
  L0R=L0F(YG2D)
  L0C11=L0F(C11)
  DO IX=IXF,IXL
  DO IY=IYF,IYL
    ICELL = IY+(IX-1)*NY
    F(LOVAL+ICELL)=(3.*rg(25)/(3.14195*(rg(26)**2)))*
    & EXP(-3*(F(L0R+ICELL)**2)/(RG(26)**2))

    F(L0C11+ICELL)=F(LOVAL+ICELL)
  ENDDO
ENDDO
ENDIF

C Gaussian current source
C RG(30)=I
C RG(31)=R= EFFECTIVE RADIUS
C RG(32)=SIGMA = ELECTRICAL CONDUCTIVITY

IF(NPATCH(1:6).EQ.'GAUSSJ') THEN
  L0R=L0F(YG2D)
  L0C19=L0F(C19)
  L0VAL=L0F(VAL)
  DO IX=IXF,IXL
  DO IY=IYF,IYL
    ICELL = IY+(IX-1)*Ny
    F(LOVAL+ICELL)=(3.*RG(30)/(3.14195*(RG(31)**2)))*
    & EXP(-3*(F(L0R+ICELL)**2)/(RG(31)**2))/RG(32)

    F(L0C19+ICELL)=F(LOVAL+ICELL)
  ENDDO
ENDDO
ENDIF

C Add Joule heating
IF(NPATCH(1:7).EQ.'LORHEAT')THEN
  IF(INDVAR.EQ.H1)THEN
    L0VAL=L0F(VAL)
    L0C17=L0F(C17)
    L0C18=L0F(C18)
    DO IX=IXF,IXL
    DO IY=IYF,IYL
      ICELL = IY + (IX-1) * NY
      F(LOVAL+ICELL)=(F(L0C17+ICELL)*F(L0C17+ICELL)+
    & F(L0C18+ICELL)*F(L0C18+ICELL))/RG(32)
    C switch on lorentz heat contribution after soln has stabilised a bit
    IF(ISWEEP.LE.50)F(LOVAL+ICELL)=0.0
  ENDDO
ENDDO
ENDIF

C Add Lorentz forces
IF(NPATCH(1:7).EQ.'LORENTZ')THEN
  IF(INDVAR.EQ.V1)THEN
    I0VAL=L0F(VAL)
    I0C17=L0F(C17)
    DO IX=IXF,IXL
    DO IY=IYF,IYL
      ICELL = IY + (IX-1) * NY
      F(LOVAL+ICELL)=F(L0C17+ICELL)
      IF(ISWEEP.LE.50)F(LOVAL+ICELL)=0.0
    ENDDO
  ENDDO
  ENDF
  IF(INDVAR.EQ.W1)THEN
    L0VAL=L0F(VAL)
    L0C18=L0F(C18)
    DO IX=IXF,IXL
    DO IY=IYF,IYL
      ICELL = IY + (IX-1) * NY
      F(LOVAL+ICELL)=F(L0C18+ICELL)
      IF(ISWEEP.LE.50)F(LOVAL+ICELL)=0.0
    ENDDO
  ENDDO
  ENDF
ENDIF

C Add Marangoni shear force
IF(NPATCH(1:3).EQ.'TAU')THEN
  L0VAL=L0F(VAL)
  L0T=L0F(INAME('TMP1'))
  L0R=L0F(YG2D)
  I0C20=L0F(C20)
  dSDT=RG(1)
  DO IX=IXF,IXL
  DO IY=IYF,INY-1
    ID=IXADD+IY
    DR=F(L0R+ID)-F(L0R+ID+1)
    DTEMP=F(L0T+ID)-F(L0T+ID+1)
    DTDR=DTEMP/DR
    F(LOVAL+ID)=DSDT*DTDR
    F(L0C20+ID)=F(LOVAL+ID)
  ENDDO
ENDDO
ENDIF

C Add radiative heat loss
IF(NPATCH(1:4).EQ.'HRAD')THEN
  DO IX=IXF,IXL
  DO IY=IYF,IYL
    ICELL = IY + (IX-1) * NY
  C RG(29) is ambient temperature
  F(LOVAL+ICELL)=RG(29)
  ENDDO
ENDDO
ENDIF

C Convective source for solidification
C
IF(NPATCH.EQ.'CON') THEN
C Get face areas these contain blockage adjustment
C
  L0AY=L0F(ANORTH)
  I0AH=L0F(AHIGH)
C Get velocities
  L0V1=L0F(V1)
  I0W1=L0F(W1)
  L0LW1=L0F(LOW(W1))
  I0LAT=INAME('LATH')
  L0LLAT=L0F(LOW(ILAT))
  I0HLAT=L0F(HIGH(ILAT))
C Calculate F's
  DO IX=IXF,IXL
  IXADD=(IX-1)*NY
  DO IY=IYF,IYL
  ID=IY+IXADD
C South face
  GFS=RHO LIQ * F(L0V1+ID-1) * F(L0AY+ID-1)
  IF(IY.EQ.1) GFS = 0.0
C North face
  GFN=RHO LIQ * F(L0V1+ID) * F(L0AY+ID)
  IF(IY.EQ.NY) GFN = 0.0
C Low face
  GFL=RHO LIQ * F(L0LW1+ID) * F(L0AH+ID)
  IF(IZ.EQ.1) GFL = 0.0
C F high is calculated to ensure continuity
  GFH=GFL+GFS-GFN
  IF(IZ.EQ.NZ)GFH=0.0
C Calculate inflows to J,I using upwind
  GINS=MAX(GFS,0.0)*F(I0LAT+ID-1)
  > -MAX(-GFS,0.0)*F(I0LAT+ID)
  GINL=MAX(GFL,0.0)*F(I0LLAT+ID)
  > -MAX(-GFL,0.0)*F(I0LAT+ID)
C
C CALCULATE OUTFLOWS TO J,IZSTEP
  GOTN=MAX(GFN,0.0)*F(I0LAT+ID)
  > -MAX(-GFN,0.0)*F(I0LAT+ID+1)
  GOTH=MAX(GFH,0.0)*F(I0LAT+ID)
  > -MAX(-GFH,0.0)*F(I0HLAT+ID)
  >
C Source is inflow-outflow
  F(LOVAL+ID)=GINL+GINS-GOTH-GOTN
  ENDDO
ENDDO
ENDIF

C Boussinesq source- z direction only
C
IF(NPATCH.EQ.'BSQ') THEN
  L0HTMP=L0F(HIGH('TEMP1'))
  DO IX=IXF,IXL
  IXADD=(IX-1)*NY
  DO IY=IYF,IYL
  ID=IY+IXADD
C Buoyancy term
C TREF: Reference temperature. Assume to be the average of liquidus and
C Solidus temperature.
  F(LOVAL+ID)=-0.5*BETA*GRVTY*RHO1*(F(L0TMP+ID)-TREF+
  & F(L0HTMP+ID)-TREF)
  ENDDO
ENDDO
ENDIF

C--- GROUP 19. Special calls to GROUND from EARTH
C * ----- SECTION 3 ---- Start of iz slab.
C Do This only for the first sweep....after use corrections
C to update the liquid fraction
  L0SOL = I0F( INAME('SOLF'))
  L0LFN = L0F( INAME('LIQF'))
  L0LAT = L0F( INAME('LATH'))

```

```

L0TMP = L0F( TEMP1 )
IF(ISWEEP.EQ.1) THEN
C DEL H BY DT, Part of Latent heat source redundant in steady state
DO IX=1,NX
  IXADD=(IX-1)*NY
DO IY=1,NY
  ID=IY+IXADD
C Latent heat update
C
  GTP=F(L0TMP+ID)
  GFTEMP = F(L0LFN+ID )
  GTRANGE = TLQUS - TSOL
  IF (GTP.LT.TSOL) THEN
    F(L0LFN+ID) = 0.0
  ELSEIF (GTP.GT.TLQUS) THEN
    F(L0LFN+id) = 1.0
  ELSE
    IF (GTRANGE.lt.1E-6) THEN
      F(L0LFN+ID) = 1.0
    ELSE
      F(L0LFN+ID) = (GTP - TSOL)/GTRANGE
    ENDIF
  ENDIF
C Different method
C
  CTOP = CPLIQ * (gTP - (TSOL + gFTEMP*(TLQUS - TSOL )))
  CBOT = gLAT + ( TLQUS - TSOL ) * CPLIQ
  FCOR = CTOP / CBOT
  GLFNEW = GFTEMP + FCOR
C end_of Different method
C
C Over/under shoot correction
  GLFNEW = MIN( 1.0, GLFNEW )
C
C Calculate solid volume fraction in cell
C
  F(L0SOL+ID)=(1. - F(L0LFN+ID))
C Calculate new Latent heat content of cell
c
  F(L0LAT+ID) = F(L0LFN+ID) * GLAT
C End_of_initial_solid_fraction_calculation_for_first_sweep

C Calculate new Latent heat content of the cell if things were transient
C
C Qlatent = rho * latent * (lfold - lf) * volume / dt
C
  DT = 1.
C
  F(L0VAL+ID)= GLAT*RHO LIQ *(GLFOLD - GLFNEW)/DT
  ENDDO
  ENDDO
ENDIF
C Correct Solid fraction for sweeps > 1st
IF(ISWEEP.GT.1)THEN
  GTRANGE = TLQUS - TSOL
  DO IX=1,NX
    DO IY = 1,NY
      ICELL = IY + (IX-1)*NY
      R_CORR_VAL = F(L0TMP+ICELL)-
(GTRANGE*F(L0LFN+ICELL)+TSOL)
C cpliq should really be cp cell BY cell liq OR solf
      RDH = GLAT/ CPLIQ + GTRANGE
      CORRH = R_CORR_VAL / MAX (RDH,1E-6)
C update liqf
      RLF = F(L0LFN+ICELL) + RG(23)*CORRH
      RLF = MIN(MAX(RLF,0.0),1.0)
      F(L0LFN+ICELL) = RLF
      F(L0SOL+ICELL) = 1. -RLF
C update Latent Heat of Cells
      F(L0LAT+ICELL) = F(L0LFN+ICELL) * GLAT
    ENDDO
  ENDDO
  ENDDO
ENDIF

```

```

C * ----- SECTION 4 ---- Start of iterations over slab.
  CALL GETZ(ZGNZ,GZG,NZ)
C * ----- SECTION 6 ---- Finish of iz slab.
C Calculate Current and magnetic field
  L0DY=L0F(DYG2D)
  L0C1=L0F(C1)
  L0C14=L0F(C14)
  L0C15=L0F(C15)
C Jr
  DO IX=1,NX
    DO IY=1,NY-1
      ICELL=IY+NY*(IX-1)
      F(L0C14+ICELL)=(F(L0C1+ICELL+1)-F(L0C1+ICELL))/F(L0DY+ICELL)
      F(L0C14+ICELL)=-RG(32)*F(L0C14+ICELL)
    ENDDO
  ENDDO
  DO IX=1,NX
    DO IY=NY,NY
      ICELL=IY+NY*(IX-1)
      F(L0C14+ICELL)=F(L0C14+ICELL-1)
    ENDDO
  ENDDO
C Jz
  IF(IZ.EQ.1)THEN
    DO IX=1,NX
      DO IY=1,NY
        ICELL=IY+NY*(IX-1)
        F(L0C15+ICELL)=0.0
      ENDDO
    ENDDO
  ENDDO
  IF(IZ.NE.1)THEN
    L0C1=ANYZ(C1,IZ-1)
    L0IC1=ANYZ(C1,IZ)
    DO IX=1,NX
      DO IY=1,NY
        ICELL=IY+NY*(IX-1)
        F(L0C15+ICELL)=-RG(32)*(F(-L0IC1+ICELL)-F(-L0C1+ICELL))/
          (GZG(IZ)-GZG(IZ-1))
      ENDDO
    ENDDO
  ENDDO
  ENDDO
C -- Calculate Magnetic Field
  L0C14=L0F(C14)
  L0C15=L0F(C15)
  L0C16=L0F(C16)
  L0C17=L0F(C17)
  L0C18=L0F(C18)
  L0YG=L0F(YG2D)
  L0DYV=L0F(DYV2D)
  RSUM=0.0
  DO IX=1,NX
    DO IY=1,NY
      ICELL=IY+(IX-1)*NY
      F(L0C16+ICELL)=rsum+RG(33)/F(L0YG+ICELL)*
        F(L0C15+ICELL)*F(L0YG+ICELL)*F(L0DYV+ICELL)
      RSUM =F(L0C16+ICELL)
    ENDDO
  ENDDO
  RSUM =0.0
  DO IX=1,NX
    DO IY=1,NY
      ICELL=IY+(IX-1)*NY
      F(L0C17+ICELL)=-F(L0C15+ICELL)*F(L0C16+ICELL)
    ENDDO
  ENDDO
  DO IX=1,NX
    DO IY=1,NY
      ICELL=IY+(IX-1)*NY
      F(L0C18+ICELL)=F(L0C14+ICELL)*F(L0C16+ICELL)
    ENDDO
  ENDDO

```